Pure and Applied Geophysics

Do Cloud Properties in a Puerto Rican Tropical Montane Cloud Forest Depend on Occurrence of Long-Range Transported African Dust?

Johanna K. Spiegel,[1] Nina Buchmann,[1] Olga L. Mayol-Bracero,[2] Luis A. Cuadra-Rodriguez,[3] Carlos J. Valle Díaz,[2,4] Kimberly A. Prather,[5] Stephan Mertes,[6] and Werner Eugster[1]

Abstract—We investigated cloud properties of warm clouds in a tropical montane cloud forest at Pico del Este (1,051 m a.s.l.) in the northeastern part of Puerto Rico to address the question of whether cloud properties in the Caribbean could potentially be affected by African dust transported across the Atlantic Ocean. We analyzed data collected during 12 days in July 2011. Cloud droplet size spectra were measured using the FM-100 fog droplet spectrometer that measured droplet size distributions in the range from 2 to 49 μm, primarily during fog events. The droplet size spectra revealed a bimodal structure, with the first peak ($D < 6$ μm) being more pronounced in terms of droplet number concentrations, whereas the second peak (10 μm $< D < 20$ μm) was found to be the one relevant for total liquid water content (LWC) of the cloud. We identified three major clusters of characteristic droplet size spectra by means of hierarchical clustering. All clusters differed significantly from each other in droplet number concentration (N_{tot}), effective diameter (ED), and median volume diameter (MVD). For the cluster comprising the largest droplets and the lowest droplet number concentrations, we found evidence of inhomogeneous mixing in the cloud. Contrastingly, the other two clusters revealed microphysical behavior, which could be expected under homogeneous mixing conditions. For those conditions, an increase in cloud condensation nuclei—e.g., from processed African dust transported to the site—is supposed to lead to an increased droplet concentration. In fact, one of these two clusters showed a clear shift of cloud droplet size spectra towards smaller droplet diameters. Since this cluster occurred during periods with strong evidence for the presence of long-range transported African dust, we hypothesize a link between the observed dust episodes and cloud characteristics in the Caribbean at our site, which is similar to the anthropogenic aerosol indirect effect.

Key words: Caribbean trade wind cumulus, fog, Saharan dust, aerosol indirect effect, tropical montane cloud forest, Caribbean.

1. Introduction

The tropical montane cloud forests (TMCF) in the northeastern part of Puerto Rico provide a perfect natural laboratory to examine the impact of one of the most abundant natural aerosols on cloud properties: African dust (AD) (e.g., Goudie and Middleton 2001). Each year in the summer months, trade winds transport AD particles to the Caribbean (Prospero and Nees 1986; Muhs et al. 1990; Prospero and Lamb 2003; Huang et al. 2010; Prospero and Mayol-Bracero 2013). Such transports have been found to be important for the geochemical cycles, radiative balance, human health, and ecosystems of the region (e.g., Muhs et al. 1990; Li et al. 1996; Shinn et al. 2000; Gyan et al. 2005; Gioda et al. 2013).

Natural and anthropogenic aerosol particles influence cloud microphysical, radiative and chemical processes in the atmosphere. Their direct effect on climate via scattering and absorption of radiation, as well as their indirect effect via cloud formation influencing Earth's albedo and cloud persistence, has received wide attention in recent years (Kaufman et al. 2002; Andreae et al. 2004; Hartmann et al. 2013; Rosenfeld et al. 2008). It is the small droplets (smaller than drizzle) that affect cloud albedo, and progress has been made in understanding these

[1] Institute of Agricultural Sciences, ETH Zürich, Zurich, Switzerland. E-mail: eugsterw@ethz.ch
[2] Institute for Tropical Ecosystem Studies, University of Puerto Rico, San Juan, Puerto Rico.
[3] Department of Chemistry, University of California, San Diego, La Jolla, CA 92093, USA.
[4] Department of Graduate Chemistry, University of Puerto Rico, San Juan, Puerto Rico.
[5] Department of Chemistry and Biochemistry and Scripps Institution of Oceanography, University of California, San Diego, La Jolla, CA 92093, USA.
[6] Leibniz Institute for Tropospheric Research, Leipzig, Germany.

effects, but predicting cloud persistence is only possible with a high level of understanding of very detailed processes (Boucher et al. 2013). Although tropical ecosystems—e.g. in the Caribbean—are supposed to react very sensitively to temperature changes, cloud–aerosol interaction studies are very rare in the Caribbean region.

TMCF are characterized by a persistent cloud and fog cover (e.g., Tanner et al. 1992; Bruijnzeel et al. 2010). Here we will use the term fog synonymously for a cloud with its base at the earth's surface and interacting with the vegetation. In Puerto Rico, Novakov et al. (1994) were the first to measure total cloud droplet number concentration, LWC_{tot} (liquid water content, which is the total mass of liquid water in cloud droplets per unit volume of air), and effective radii at the El Yunque mountain site in 1992. They observed a barely significant ($p < 0.2$) dependence of droplet number concentration on non-sea-salt sulfate concentration for part of the measured clouds. Entrainment and mixing processes were suggested, as explanations for this low sensitivity of cloud droplet number concentration with respect to aerosol number concentration. In 2004, the Rain in Cumulus Clouds Over the Ocean—Puerto Rico Aerosol Cloud Interaction Study (RICO-PRACS) followed with measurements at Pico del Este (Allan et al. 2008; Gioda et al. 2008). A relationship was found between prevailing wind direction (ESE to ENE) and cloud properties based on a 7-day observation period in December 2004, with droplet spectra measured during daytime hours. Droplet number concentrations and LWC_{tot} were higher, while median volume diameter (MVD) was lower when the air mass arrived from the ESE in comparison to the ENE sector. The authors attributed these differences to changes in aerosol number concentration and properties due to additional anthropogenic pollution when the wind came from ESE. The only characterization of cloud properties and water fluxes in TMCF near the top of Pico del Este in Puerto Rico based on continuous measurements was done in summer 2002 during a 43-day observation period, but without considering the possible relevance of the AD component (Eugster et al. 2006). Fog occurred during 85 % of the time and only tended to disappear around noon (local time) as a consequence of ascent of the

marine boundary layer or synoptic weather events (Holwerda 2005; Eugster et al. 2006). Consequently, the LWC_{tot} and the volume weighted mean diameter also followed a diel cycle, with lowest values around noon ($\approx$5 mg m^{-3} and $\approx$8 μm, respectively), and highest values at night ($\approx$100 mg m^{-3} and $\approx$15 μm, respectively). This diel pattern found at Pico del Este is typical for weather conditions in a tropical climate (e.g., Brown et al. 1983; Holwerda 2005).

African Dust (AD) is one of the most abundant types of natural mineral aerosols in the atmosphere (e.g., Goudie and Middleton 2001). Dust storms in the Sahara desert or the Sahel remove dust particles from the surface and convectively lift it to higher atmospheric levels. AD particles can then be transported to Europe (e.g., Ansmann et al. 2005; Coz et al. 2010), or, depending on the season, can be transported by trade winds across the Atlantic Ocean to South America and the Gulf of Mexico (Colarco et al. 2003; Maring et al. 2003; Prospero and Lamb 2003; Bristow et al. 2010; Huang et al. 2010; Prospero et al. 2010; Prospero and Mayol-Bracero 2013). The physical properties of dust strongly depend on its mineral composition, which has been characterized in many studies near the source (Chou et al. 2008; Formenti et al. 2008; Kandler et al. 2009). Based on laboratory studies, mineral dust particles are commonly believed to be good ice nuclei (Field et al. 2006; Kanji and Abbatt 2006; Lüönd et al. 2010). However, recently, the hygroscopicity of dust—the ability of dust to take up water—has received more attention. During extended transport phases (i.e., across the Atlantic Ocean), gaseous species can condense on dust particle surfaces, leading to liquid or soluble coatings (Levin et al. 1996, 2005; Laskin et al. 2005; Li and Shao 2009; Matsuki et al. 2010; Takahama et al. 2010). These processes are summarized by the term "aging of dust". While laboratory studies showed that pure dust has a low hygroscopicity, the occurrence of small amounts of soluble materials on the dust surface can enhance its hygroscopic behavior (Gustafsson et al. 2005; Gibson et al. 2006; Kelly et al. 2007; Herich et al. 2009). However, aging alone does not always increase the hygroscopicity of dust: Sullivan et al.

(2009) showed that calcium sulphate and calcium oxalate, which are ubiquitous components used as a proxy for aged mineral dust, remained non-hygroscopic even when aged. Hence, our best understanding is that both the mineralogical composition of aerosols and its secondary components—which can coat dust particles during long-range transport, e.g., as a result of heterogeneous chemical reactions—may control the cloud condensation nuclei (CCN) activity of dust.

Different mechanisms describing how dust could affect cloud properties have been proposed:

1. On the one hand, an increase in transported aged dust particles can lead to increased numbers of CCN, resulting in clouds with smaller, but more numerous droplets, similar to the anthropogenic direct aerosol effect (ROSENFELD et al. 2001; KELLY et al. 2007).
2. On the other hand, large aged dust particles could serve as giant CCN, provided they survive the Atlantic passage. Larger droplets grow rapidly at the expense of smaller droplets, which would lead to a droplet size spectrum with larger, but fewer, droplets (LEVIN et al. 1996).
3. However, if aging of dust did not enhance its ability to act as CCN (SULLIVAN et al. 2009), droplet size spectra in clouds and fog should be unaffected by the presence or absence of AD, although the number concentrations of aerosol particles could rise enormously when dust is present.

In theory, all these possibilities are realistic for AD arriving in the Caribbean. It is therefore a priori not clear if and how droplet size distributions in a Puerto Rican cloud forest are affected by long-range transported dust.

In this study, we ask the question of whether observed variations in cloud properties are linked to events with long-range transported AD. We present the first detailed analysis of the cloud properties in a TMCF in Puerto Rico based on in situ measurements. The main goal was to determine whether such in situ measurements at a representative mountain in the Caribbean are able to support the hypothesis that AD transport across the Atlantic has an influence on cloud properties, which in turn could lead to a feedback to climate via the modification of the cloud–albedo feedback process.

2. Materials and Methods

2.1. Research Site and PRADACS Field Campaign

Cloud droplet size spectra were measured at Pico del Este (PE, 18°16.21′N, 65°45.57′W, 1,051 m a.s.l.) in the northeastern part of Puerto Rico, around 20 km from the Atlantic coast during the Puerto Rico African Dust And Clouds Study (PRADACS) field campaign in summer 2011. For two reasons, PE is an excellent place to study the impact of aged dust on cloud properties: First, PE is frequently immersed in clouds, a consequence of the orographically induced lifting and hence cooling of the humid air masses advected by the northeasterly trade winds from the Atlantic Ocean, leading to the formation of TMCF (BAYNTON 1969; GARCIA-MARTINO et al. 1996; HOLWERDA et al. 2006; BRUIJNZEEL et al. 2010). Second, in the summer months, the site receives AD plumes that are transported across the Atlantic Ocean by the trade winds (PROSPERO AND NEES 1986; MUHS et al. 1990; PROSPERO AND LAMB 2003; HUANG et al. 2010). Although southeasterly winds advect air from the smaller islands upwind of Puerto Rico, which may be slightly polluted by anthropogenic emissions, the prevailing wind directions from the northeast transport air masses to PE that can normally be considered to be clean (ALLAN et al. 2008).

The aim of the PRADACS project was to investigate physical and chemical properties of the long-range transported AD and to quantify its impact on clouds in the TMCF. PRADACS consists of two intensive field campaigns in August 2010 and June–September 2011. Here we present a case study when data were collected from 1–12 July 2011, during which the data quality was adequate to address our research question.

2.2. Instrumentation

A high-speed cloud droplet spectrometer (FM-100, Droplet Measurement Technologies Inc., Boulder, CO, USA; see e.g., BURKARD et al. 2002; EUGSTER

et al. 2006; SPIEGEL et al. 2012) was used to measure the size spectrum of cloud droplets. The instrument was mounted ≈3 m above ground level on a scaffolding tower close to the field container. The inlet of the FM-100 was oriented towards 58° (NE) to face the mean wind direction expected during this time of the year (GARCIA-MARTINO et al. 1996). Droplets were sized by means of forward light scattering, and were recorded in 40 size bins covering the diameter range of ≈2–49 μm. It would be interesting to know the full size range from small droplets up to drizzle and light precipitation (GULTEPE 2008), beyond the upper threshold of 49 μm imposed by the FM-100. However, TWOMEY (1977) have shown that cloud surface albedo primarily depends on the droplet size numbers, not liquid water content (for which the large droplets are key), and hence the quantification of the smallest droplet sizes, which are also the ones with the highest number concentrations in clouds, is the key for addressing the question of whether cloud properties depend on dust loads. The 40 size bins have been optimized according to the Mie scattering curve as suggested by SPIEGEL et al. (2012). For details on the measurement principle, we refer to SPIEGEL et al. (2012).

In order to correct for droplet losses due to non-isoaxial and non-isokinetic sampling, we measured the wind vector next to the FM-100 inlet, using a three-dimensional (3D) ultrasonic anemometer (with integrated inclinometer; Solent HS, Gill Ltd., Lymington, UK) mounted at 0.5 m vertical distance from the FM-100 inlet. Both instruments were installed stationary and operated at a data-recording rate of 12.5 Hz (for details see EUGSTER et al. 2006). Horizontal wind direction and inclination angle represent one-minute averages computed from the mean 3D wind vector. Temperature, air pressure and rain were recorded by a Vantage Pro weather station (Davis Model 6160C) installed within 100 m from the FM-100.

In order to identify the presence of AD periods at the measurement site, the following instruments and data sets were used:

– A portable aerosol time-of-flight mass spectrometer (ATOFMS, see for details GARD et al. 1997) was deployed at PE in the framework of

PRADACS to characterize the chemical composition of individual aerosol particles and to distinguish between periods of dust, pollution, and marine influences.

– Aerosol optical depth (AOD) measurements from the MODIS satellite (ZHANG and REID 2006; SHI et al. 2011).

– Ground-based sun photometer measurements performed at Cape San Juan, around 20 km NW of PE, and at La Parguera at 130 km WSW of PE (http://aeronet.gsfc.nasa.gov/new_web/data.html).

2.3. Data Processing and Deduced Cloud Characteristics

Cloud droplet size spectra were averaged every minute and corrected for the Mie scattering uncertainties and for particle losses as proposed by SPIEGEL et al. (2012). After correction, droplet size spectra resolved diameters ranging from 2 to 49 μm, distributed over 24 bins, with a bin width of $\Delta d_i = 2\,\mu m$, where d_i is the geometric mean diameter of each bin.

From the corrected cloud size spectra, we deduced the following variables to characterize a cloud:

– Total droplet number concentration N_{tot} (cm^{-3}) and droplet number concentration per micrometer n_i ($cm^{-3}\,\mu m^{-1}$):

$$N_{tot} = \sum_{i=1}^{24} n_i\, \Delta d_i \quad \text{with} \quad n_i = \frac{\Delta N_{tot}}{\Delta d_i} \qquad (1)$$

– Total liquid water content LWC_{tot} ($mg\,m^{-3}$), as well as liquid water content per particle size bin, lwc_i ($mg\,m^{-3}\,\mu m^{-1}$):

$$LWC_{tot} = \sum_{i=1}^{24} lwc_i \Delta d_i \quad \text{with} \quad lwc_i = \frac{1}{6}\,\pi\, d_i^3\, n_i\, \rho_{H_2O},$$
$$(2)$$

where ρ_{H_2O} denotes the density of water ($kg\,m^{-3}$)

– Effective diameter ED (μm) is the droplet diameter that has the same volume-to-surface ratio as the measured spectrum:

$$ED = \frac{\sum_{i=1}^{24} d_i^3\, n_i\, \Delta d_i}{\sum_{i=1}^{24} d_i^2\, n_i\, \Delta d_i} \qquad (3)$$

– Median volume diameter MVD (µm) is the droplet diameter that divides the total volume of the droplet spectrum in two halves with equal volume:

$$\text{MVD} = b_k + \left(\frac{0.5 - \text{cum}_{k-1}}{\frac{\text{lwc}_k}{\text{LWC}_{\text{tot}}}} \right)(b_{k+1} - b_k), \quad (4)$$

where b_k is the lower boundary of bin k, and with

$$\text{cum}_k = \sum_{i=1}^{k} \frac{\text{lwc}_i}{\text{LWC}_{\text{tot}}} \Delta d_i, \quad (5)$$

where $k \in [1, 24]$ is defined as the bin number in which the MVD is found, and hence $\text{cum}_k > 0.5$, and $i \in [1, k]$.

To identify variations in the droplet size spectra that might be linked to AD, we used an indirect approach. We first searched for cloud droplet size spectra with similar features using conventional hierarchical cluster analysis, and then tried to attribute the different groups (i.e., clusters) of cloud spectra to possible driving forces. Cluster procedures categorize data points by forming groups ("clusters"). A hierarchical clustering procedure finds clusters in which the members of inferior-ranking clusters become members of larger, higher-ranking clusters (LEGENDRE and LEGENDRE 1998, Chapter 8). By doing so, we were able to avoid using our expectations for the grouping of the events, which could have missed relevant features. The grouping via hierarchical clustering was done with Ward's minimum variance method using hourly means of the droplet size distributions. This method aggregates groups by minimizing the within-group variance (WILKS 2006).

Time series of hourly means of droplet size distributions are serially auto-correlated, which means that data obtained during one hour are not independent of data measured during the previous hour. To correct for such serial auto-correlation in statistical comparisons between clusters, we used the WILKS (2006) variance inflation correction approach: the number of independent data points m' in a time series belonging to a specific cluster was derived from the number of measured data points m corrected via the lag-1 auto-correlation coefficient ρ_1: $m' = m \cdot (1 - \rho_1)/(1 + \rho_1)$. In the special case of absence of serial auto-correlation, $\rho_1 = 0$ and hence, $m' = m$. Then we compared the mean values of the different clusters using Tukey's honest significant differences (HSD) test using m' as the number of independent values in the statistical test. Tukey's HSD test adjusts significance levels for multiple testing. This is a standard procedure to account for the increasing probability that multiple testing can lead to randomly occurring significant comparisons (false positives).

2.4. Idealized Droplet Size Distributions

In order to compare droplet size distributions more quantitatively, we fitted the sum of two scaled log-normal distributions (F) to the measured median droplet distributions by means of least squares fitting:

$$F = x_{1,\log}(D) + x_{2,\log}(D), \quad (6)$$

where D is the median droplet diameter of the measurements in µm. The individual density functions that are added in Eq. (6) with $i = 1, 2$ are

$$x_{i,\log}(D) = \frac{X_{i,\log}}{\sqrt{2\pi}\sigma_{i,\log}D} \exp\left\{ \frac{-\left[\ln\left(D/D_{i,\log}\right)\right]^2}{2\sigma_{i,\log}^2} \right\}, \quad (7)$$

where $X_{i,\log}$ is a scaling factor, $D_{i,\log}$ is the median diameter per mode and $\sigma_{i,\log}$ is the logarithmic width of the distribution i.

3. Results

3.1. Cloud Characteristics at Pico del Este

Data coverage of the field campaign from 1 July 2011 (00:00 UTC) to 12 July 2011 (23:59) was 73 % (209 h). During the measurement time, the site received air masses from two different mean flow directions: from east-northeast (ENE $\approx 84°$, which was further east than initially expected) and from east-southeast (ESE $\approx 110°$, Fig. 1a). Due to orography, these two different flow directions were also characterized by two different vertical wind components. For the ENE wind directions, the vertical component was higher than for ESE winds (Fig. 1b, c). This
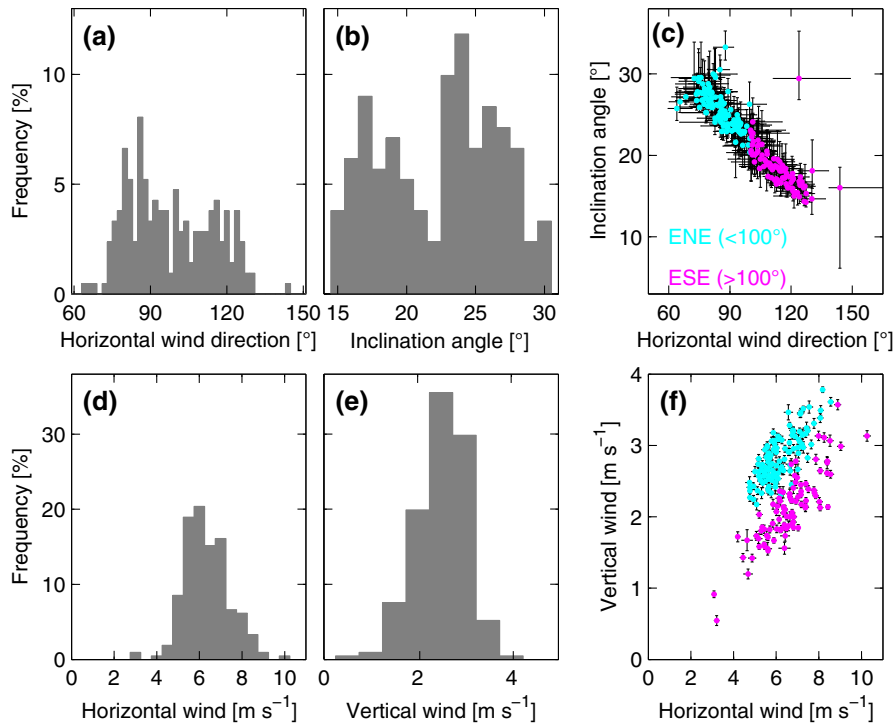
Figure 1
Wind conditions at Pico del Este, Puerto Rico (1–12 July 2011): histogram of horizontal wind direction (**a**), vertical wind direction (**b**), horizontal wind speed (**d**) and vertical wind speed (**e**) based on hourly mean values. Horizontal wind direction and inclination angle of the 3D wind vector were measured with a 3D ultrasonic anemometer using an unrotated coordinate system, where the vertical is aligned with the gravity vector of the earth. Positive vertical wind directions indicate upslope wind movements. The relationship between horizontal and vertical wind directions (**c**) is related to the topography at Pico del Este, which also reflects the two distinct regimes (ESE vs. ENE winds) of vertical versus horizontal wind speed (**f**)

pattern is also visible in wind speeds, with generally lower vertical wind speeds for the ESE sector, but comparable wind speeds for the horizontal component (Fig. 1e). No diel trend was seen in the horizontal or vertical wind speeds and horizontal wind direction. Similarly, N_{tot} was independent of collection time during the day (Fig. 2a). However, some of the cloud characteristics were subject to a diel trend: LWC_{tot}, MVD and ED were smallest at noon and highest at night (Fig. 2b–d). Thus, during the field campaign, we basically measured foggy conditions during the entire day, but fog tended to have a smaller LWC_{tot} with smaller droplets during daytime compared to night-time. A rising cloud level, which is able to explain this feature was already observed by EUGSTER et al. (2006). Consequently, we measured closer to the cloud base during the day than at night. Hence, the higher LWC_{tot} and ED as well as rather constant N_{tot} during night compared to daytime represent the corresponding

vertical gradients of cloud properties. In comparison to the RICO-PRACS study, conducted at the same location, but during a different time of the year [December 2004; ALLAN et al. (2008)] when AD transport events are unlikely, we measured smaller N_{tot}, but larger droplets as reflected by larger LWC_{tot}, ED and MVD. This may result from seasonal differences in cloud properties, but also from differences in instrumentation and data processing.

3.2. Identification of Three Characteristically Different Droplet Size Distributions

The cluster analysis revealed three major clusters of droplet size distributions (Fig. 3), with higher similarity between clusters 1 and 2 in comparison with cluster 3. The most frequent cluster was cluster 2 (51.2 % of the time, 107 h), followed by cluster 3 (35.4 %, 74 h) and the less frequent cluster 1 (13.4 %, 28 h). While
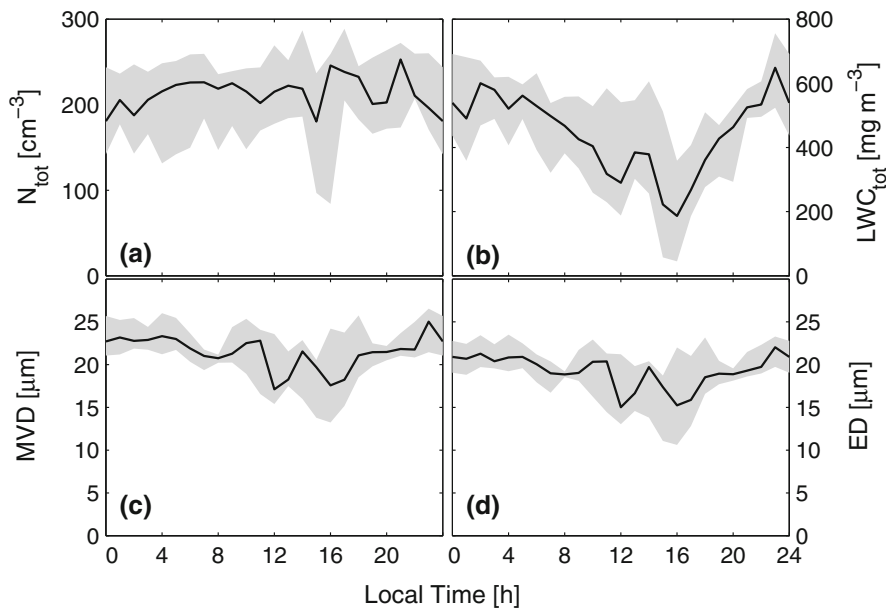
Figure 2
Median diel cycle (*black line*) of (**a**) droplet number concentration N_{tot}, (**b**) liquid water content LWC$_{tot}$, (**c**) median volume diameter MVD, and (**d**) effective diameter ED based on hourly mean values measured in July 2011 in the droplet size range 2–49 μm. The *shaded area* indicates the inter-quartile range of hourly mean values

Figure 3
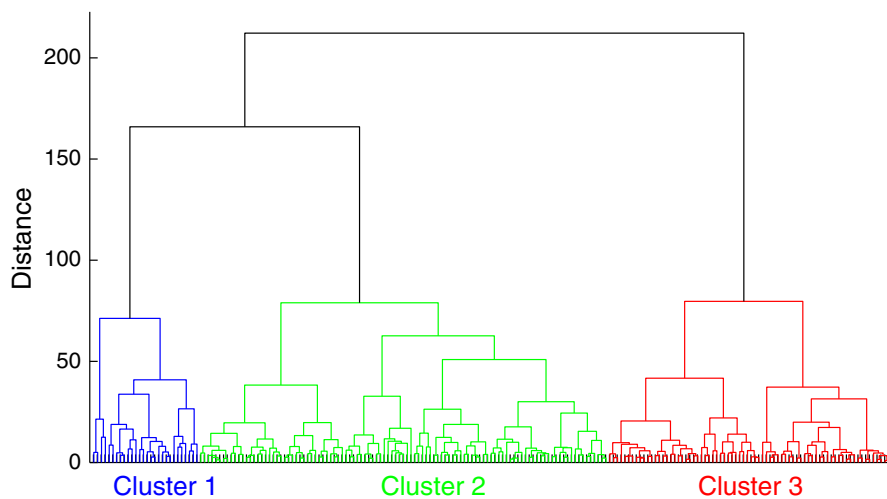Dendrogram of the hierarchical clustering of 1-h averaged droplet size spectra measured at Pico del Este, Puerto Rico (1–12 July 2011). *Each tick* on the *x* axis represents one hourly mean droplet size distribution in 24 size classes ranging from 2 to 49 μm. On the *y* axis, the distance (in the 24-dimensional space) between the 209 droplet size distributions is depicted. The height of the joint between two clusters is proportional to the distance between these clusters. The lower the joint height, the higher the similarity between the two droplet size distributions. The three clusters used in this study are marked with *different colors*

clusters 2 and 3 appeared in events of up to 20 h duration, cluster 1 contains events that persisted only for 1–3 h, except on 9 July 2011 (Fig. 4), when cluster 1 lasted from 6:00 to 21:00 (only interrupted by 2 h where data are missing due to technical problems). All three clusters are characterized by a bimodal droplet size distribution (Fig. 5; Table 1), often attributed to mixing effects (WARNER 1969).
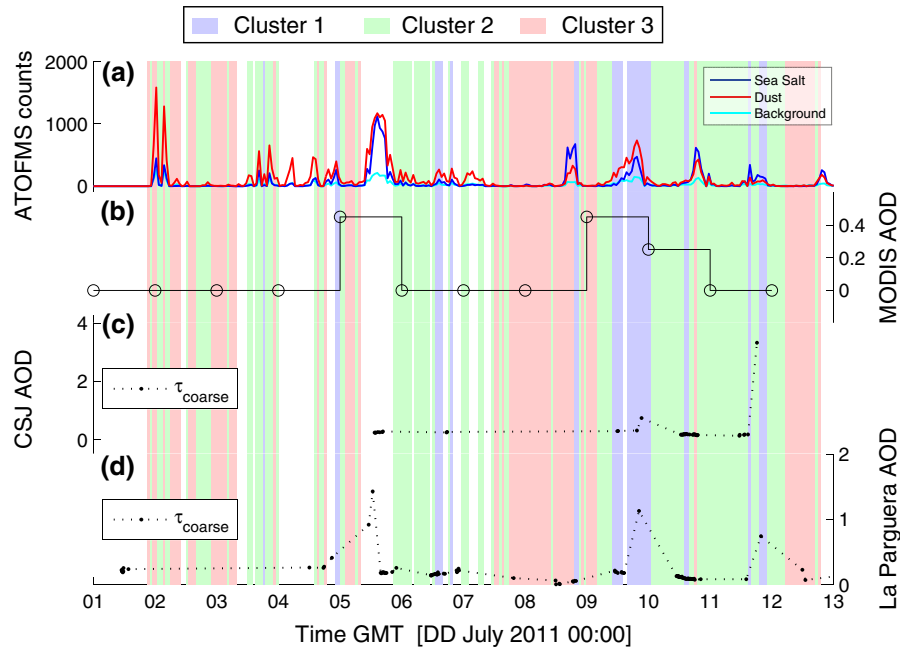
Figure 4
Time series of the three different clusters (*blue* cluster 1, *green* cluster 2, *red* cluster 3, *white* data are missing) including different indicators for the presence of long-range transported African dust (AD) in Puerto Rico. (**a**) ATOFMS counts for sea salt (*blue*) and dust (*red*); (**b**) aerosol optical depth (AOD) for 0.55 μm retrieved from MODIS satellite data; (**c**) AOD for coarse mode particles from the sun photometer at Cape San Juan, 20 km NE of Pico del Este; (**d**) AOD for coarse mode particles from the sun photometer at La Parguera, 130 km WSW of Pico del Este
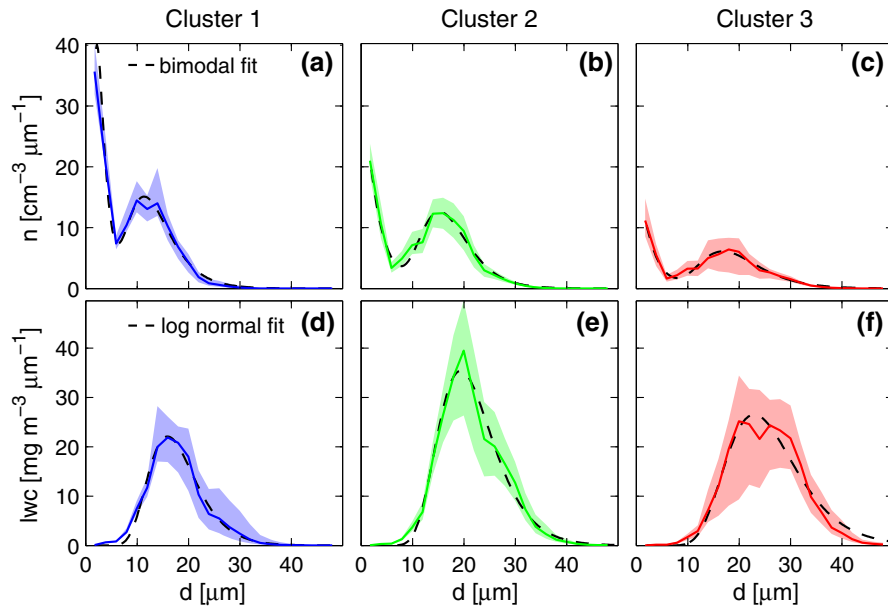

Figure 5
Median droplet size distributions (**a–c**) and liquid water content distributions (**d–f**) for the three clusters (*bold colored lines*) as well as the inter-quartile range (*shaded areas*). The *dashed black line* depicts the bimodal log-normal fit (Eq. 7) of the droplet size distribution (**a–c**) and the unimodal log-normal fit of the liquid water content distribution (**d–f**), using the parameter estimates tabulated in Table 1

Variable	Cluster	$D_{1,log}$	$\sigma_{1,log}$	$X_{1,log}$	$D_{2,log}$	$\sigma_{2,log}$	$X_{2,log}$
N_{tot}	1	2.8	0.5	121.3	13.0	0.4	160.5
	2	2.8	0.9	96.3	16.8	0.3	142.3
	3	2.7	0.9	48.7	19.0	0.3	88.7
LWC_{tot}	1	–	–	–	17.3	0.3	264.4
	2	–	–	–	20.9	0.3	492.8
	3	–	–	–	25.0	0.3	464.7

LWC_{tot} shows a unimodal distribution related to the second peak of droplet sizes (larger droplets); hence, no fit for the first distribution is given. See text for details

The FM-100 instrument cannot detect and characterize droplets that are smaller than $\approx 2\ \mu m$. Hence, in Fig. 5a–c, it remains unknown at which exact droplet size the maximum droplet number concentrations actually occurs in the first mode of the bimodal droplet size distribution. Nevertheless, the log-normal fit matches the measured data very well (Fig. 5a–c), and hence the quality of the parametric size distributions used for comparing the three clusters appears to be sufficient to reliably detect differences. The median diameter $D_{1,log}$ of the first mode was similar for all three clusters, while the scaling factor $X_{1,log}$ decreased from the first to the third cluster, indicating that the number of droplets with a diameter below 6 μm was highest for cluster 1 and smallest for cluster 3. The peak of the second mode moved towards larger droplet sizes from cluster 1 to 3, and was highest for the first cluster and smallest for the last cluster, reflected in a decreasing $X_{2,log}$ from cluster 1 to 3 and an increasing $D_{2,log}$. Because the smallest droplets have a very low volume compared to the larger droplets in the second mode of the droplet size distribution, the first mode completely disappears in the size distribution of LWC_{tot} (Fig. 5d–f). Based on the definition of the log-normal distribution, the fitting parameters $X_{2,log}$ and $D_{2,log}$ correspond to LWC_{tot} and MVD, respectively, indicating that the median of the LWC_{tot} distribution (MVD) increased slightly from cluster 1 to 3 (Fig. 6c). Especially for clusters 2 and 3, the LWC_{tot} is higher and N_{tot} slightly lower than what was measured in earlier studies at the same site. The reason

for this is that to the best of our knowledge, this is the first study in which measurements were corrected for droplet losses during the measurement process. This is especially important for the LWC_{tot} measurements, which are dominated by larger droplets that are most strongly affected by such a correction (SPIEGEL et al. 2012). But it is also well known that averaging times are important in cloud studies, since longer averaging periods relate to larger spatial scales, and hence the presence of clear patches in the clouds reduces the average droplet number concentrations (GULTEPE and ISAAC 1999). Besides the increase in LWC_{tot}, ED increased from cluster 1 to 3 (Fig. 6d), while N_{tot} decreased (Fig. 6a). Tukey's HSD test identified significant differences among all three clusters ($p < 0.05$) for N_{tot}, MVD, and ED. Contrastingly, LWC_{tot} did not differ between clusters 2 and 3, but cluster 1 had significantly lower LWC_{tot} than the other two clusters.

There was no significant difference among the clusters with respect to the horizontal wind direction (Fig. 6e), and only cluster 3 had a significantly smaller vertical wind component than clusters 1 and 2 (Fig. 6f). The total amount of rain during the occurrence of cluster 3 was twice the value observed in cluster 2, and nearly no rainfall was measured during the occurrence of cluster 1 (Table 2). The different amounts of rain might be caused by the droplet size distributions, as clouds with larger droplets are known to precipitate faster than others. This agrees with our observations as cluster 3 was the cluster with the largest droplets (Fig. 6) and highest rainfall intensities (Table 2).

Cluster 1 differed from clusters 2 and 3 in terms of its diel frequency of occurrence (Fig. 7). While the occurrence of clusters 2 and 3 was distributed similarly over the day, cluster 1 only occurred during daytime, which is when the LWC_{tot} was smallest (Fig. 2b). This diel dependence of cluster 1 was most likely the reason for the lowest LWC_{tot} and its significant difference compared to clusters 2 and 3.

3.3. Link Between Cloud Droplet Distribution and Dust Events

The appearance of cluster 1 agreed with periods when dust aerosol number concentrations as
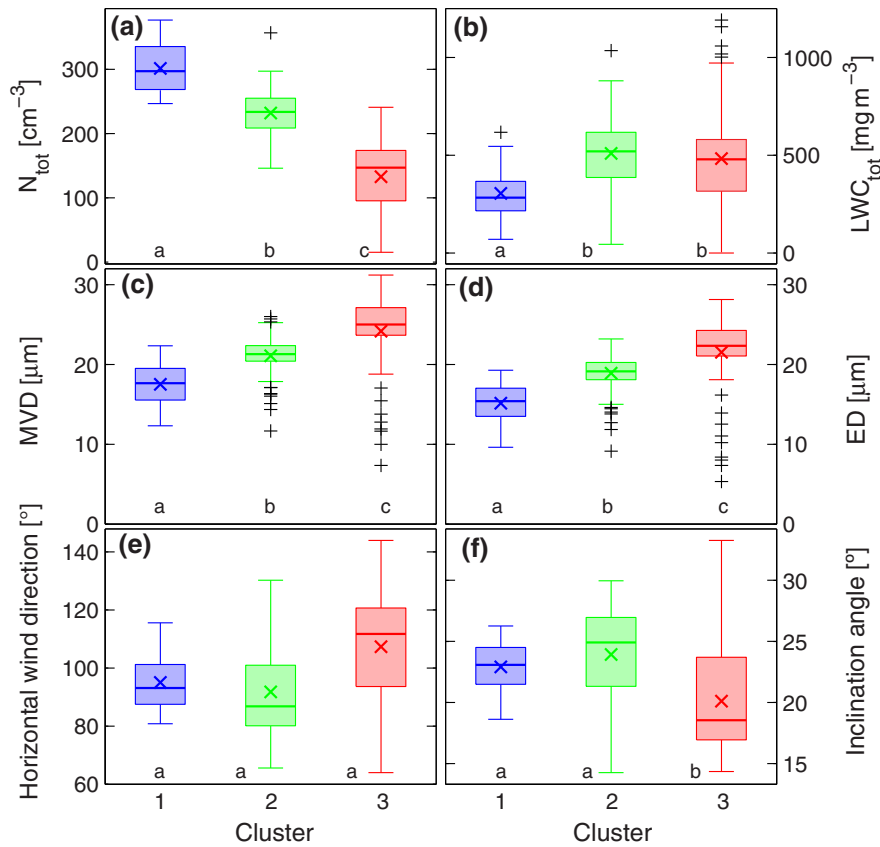
Figure 6
Boxplots of the three clusters using hourly mean values of (**a**) the droplet number concentration N_{tot}, (**b**) liquid water content LWC_{tot}, (**c**) median volume diameter MVD, (**d**) effective diameter ED, (**e**) horizontal wind direction, and (**f**) inclination angle. *Each box* comprises the median (*thick horizontal line*), the mean (*colored cross*), and the inter-quartile range (*shaded area*).The *whiskers* show the full data range up to a maximum of 1.5× the interquartile range. Data points outside that range are termed outliers (+). *Different letters* denote significant differences at $p < 0.05$

Table 2

Total amount of rainfall as well as mean rainfall intensity measured with a Davis Vantage Pro rain gauge, within 100 m distance from the fog droplet size distribution measurements during the occurrence of each cluster

Cluster	Total rainfall (mm)	Rainfall intensity (mm h^{-1})
1	3	0.028
2	41	0.38
3	89	1.2

Besides the inaccuracy of such a sensor, scale effects due to spatial variations in precipitation should be considered when interpreting these data [see e.g., HOLWERDA *et al.* (2006)]

measured by the ATOFMS exceeded those of sea salt, and both were well above background concentrations (e.g., on 9 July 2011, Fig. 4a). Also, orange colored dust deposition was observed in cloud water samples collected simultaneously with ATOFMS and FM-100 measurements. ATOFMS counts of dust and sea salt aerosols during the appearance of cluster 2 were lower than those of cluster 1, especially on 10 and 11 July. Conversely, the increased aerosol optical depth of coarse-mode aerosols measured at Cape San Juan and La Parguera on 9 July (Fig. 4c, d) agrees with dust recorded at PE.

It is highly probable that the measured dust does not originate from a local source, but rather was transported over the Atlantic, as time series of AOD measurements from the MODIS satellite for an area including Puerto Rico confirm (Fig. 4b). HYSPLIT back-trajectories (not shown) arriving on 9 July show
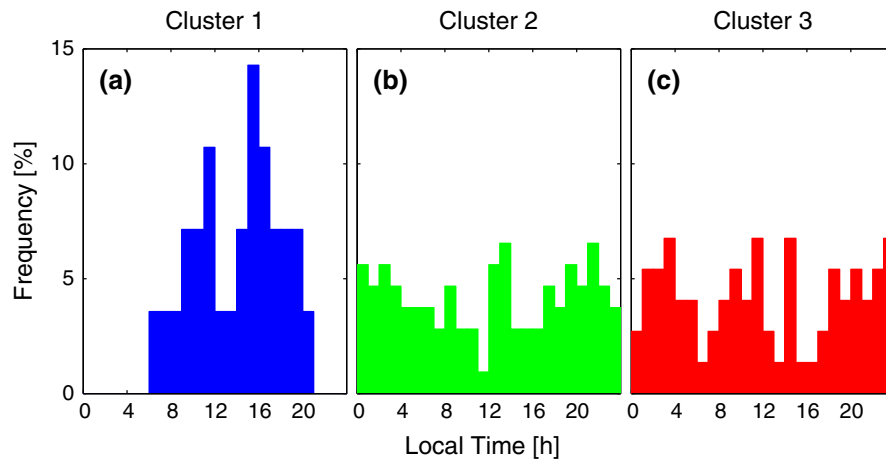
Figure 7
Diel frequency of occurrence of the three clusters (1–12 July 2011) determined from 1-h averaged data

air masses from Africa, with trajectories passing south of the Sahara across the southern Sahel.

4. Discussion

Only two studies had previously attempted to assess the cloud–aerosol interactions in Puerto Rico (NOVAKOV et al. 1994; ALLAN et al. 2008), and they reached different conclusions: ALLAN et al. (2008) found that changes in cloud microphysical behavior were mainly linked to changes in aerosol number concentrations and aerosol properties, whereas NO-VAKOV et al. (1994) only found a very weak sensitivity of droplet number concentrations on CCN concentrations, most probably due to entrainment and mixing processes in the clouds.

If AD particles become good CCN during the atlantic passage due to processing, then the idea that cloud properties in Puerto Rican TMCF do respond to AD transport can be supported with the study by ALLAN et al. (2008). Based on the study by NOVAKOV et al. (1994), a response of cloud properties to AD in Puerto Rico would additionally depend on the mixing processes in these clouds, because cloud microphysics are closely related to the question of whether condensation or mixing is the dominant process. We will therefore compare our results with these earlier studies with respect to environmental conditions, and then address the question of mixing processes in order to draw conclusions for the impact of AD.

4.1. Cloud Properties and Wind Direction

A dependency of cloud properties on prevailing wind direction was reported by ALLAN et al. (2008). They observed smaller droplet sizes, but larger droplet number concentrations and higher LWC_{tot} when the wind was coming from the ESE, and larger droplet sizes but a smaller droplet number concentration and smaller LWC_{tot} when the prevailing wind direction was ENE. They identified additional CCN from anthropogenic pollution in the ESE sector, originating from smaller populated islands along the air mass trajectory, as the main reason for this behavior.

Interestingly, prevailing wind direction, and thus air pollution, is unlikely to explain the observed differences in cloud properties of our three clusters, because all clusters cover very similar wind directions. The spread in horizontal wind directions is large, and the mean values of the wind direction do not differ significantly among the clusters (Fig. 6e). Due to the orography, the significantly smaller vertical wind component of cluster 3 (Fig. 6f) can be seen as an indication of a more southeasterly dominated and—according to ALLAN et al. (2008)—more polluted air mass during the appearance of cluster 3. However, cluster 3 has the largest droplets, but the lowest number concentrations, which is opposite to the cloud properties under ESE flow conditions observed by ALLAN et al. (2008). Hence, we conclude that the differences in cloud properties
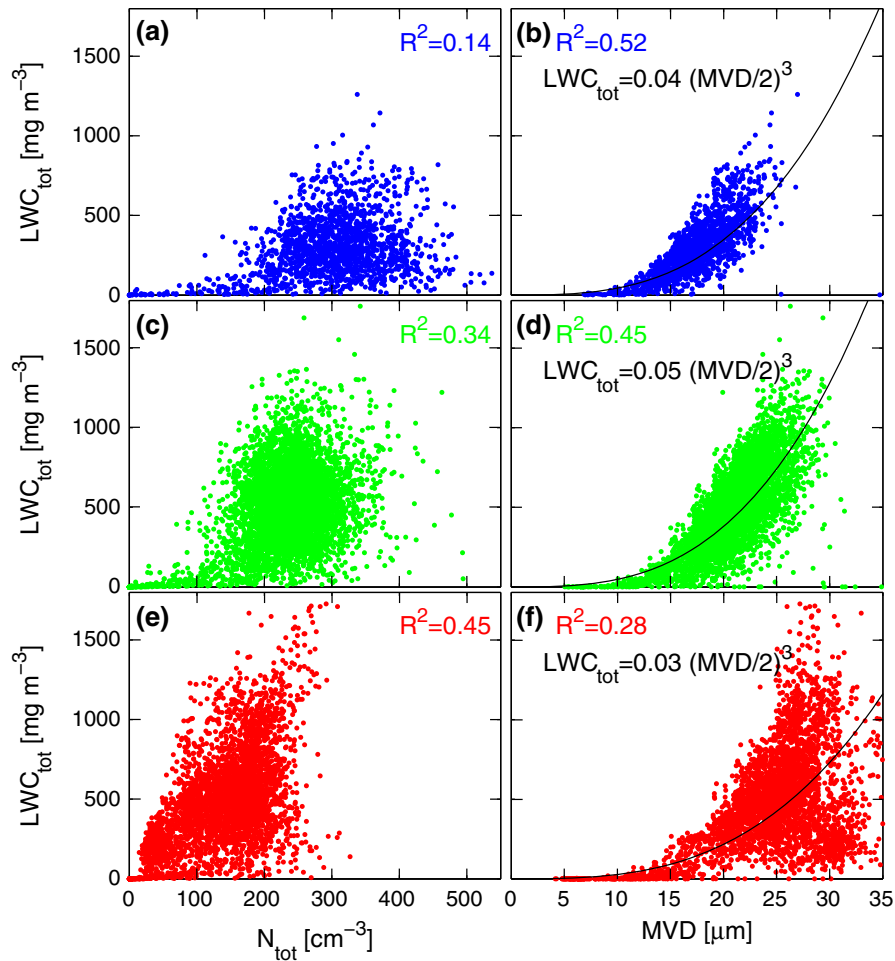
Figure 8

Correlation between 1-min averaged LWC_{tot} (liquid water content) and N_{tot} (droplet number concentration) (**a**, **c**, **e**) and between LWC_{tot} and median volume diameter (MVD) (**b**, **d**, **f**) as measured by the FM-100 fog droplet spectrometer for the three different clusters (*top* cluster 1; *center* cluster 2; *bottom* cluster 3). Data were collected between 1 and 12 July 2011. The coefficient of determination is shown in color in all panels. Least-squares fits are shown for the power law in $LWC_{tot} \sim$ MVD panels. For interpretation and a detailed description, we refer to Sect. 4.2. Note that in contrast to the previous figures, 1-min mean values are used in this comparison, as a higher time resolution is needed to clearly see the respective correlations. This also implies higher LWC_{tot}, which are reasonable and have been measured at other stations before (SPIEGEL *et al.* 2012)

of the three clusters are most likely caused by something other than differences in wind directions. In the next section, we therefore examine the mixing behavior of the three clusters.

4.2. Mixing and Entrainment

The effect of mixing on droplet spectra is complex, and has recently been addressed in a review by DEVENISH *et al.* (2012). For a quantitative analysis

of the mixing in clouds, additional measurements at different cloud heights would be needed. Unfortunately, such measurements are not available from PRADACS, and hence we had to use a more simplified approach, similar to the one presented by NOVAKOV *et al.* (1994), to qualitatively address the question of mixing and entrainment for our three cloud clusters.

In an ideal adiabatic cloud model, all cloud droplets of a spectrum experience the same

supersaturation history along their trajectory from the cloud base to the measurement point. However, due to mixing and entrainment, a measured cloud spectrum contains droplets with very different pathways through the cloud, leading to a broader cloud spectrum than expected from purely adiabatic cooling. Depending on the timescales of turbulent mixing and thermodynamic changes of the droplet (evaporation and condensation), mixing is either inhomogeneous or homogeneous. At the inhomogeneous limit, droplet number concentrations decrease, but droplet sizes stay constant. Hence, rapid changes in LWC_{tot} are basically a result of changes in droplet numbers. Thus, inhomogeneous mixing should be expressed by a good correlation between LWC_{tot} and N_{tot}. In cluster 3, this correlation is higher than in clusters 1 and 2 (Fig. 8), suggesting that cluster 3 describes the typical cloud droplet size distribution of an inhomogeneously mixed cloud at PE. On the other hand, under homogeneous mixing conditions, changes in LWC_{tot} are caused by changes in droplet diameter. Consequently, homogeneously mixed clouds are best characterized by a good correlation between LWC_{tot} and MVD. This was observed in clusters 1 and 2. In these cases, LWC_{tot} increases according to a $(MVD/2)^3$ power law (Fig. 8).

NOVAKOV et al. (1994) found a linear relationship between LWC_{tot} and N_{tot} for cumulus clouds, which are dominated by inhomogeneous mixing. In these clouds, the available number of CCN did not influence the droplet number concentration. This compares best with cluster 3 in our study. In contrast to cluster 3, clusters 1 and 2 more likely reflect homogeneously mixed clouds. Hence, our best interpretation is that clouds in clusters 1 and 2 are more likely to react to changes in aerosol concentration than those in cluster 3. This could also be the reason why clusters 1 and 2 were more closely related according to the cluster analysis (Fig. 3), with cluster 3 being more distinct. In summary, the differences between cluster 3 and the two other clusters are most likely due to different cloud dynamics, with cluster 3 representing conditions where an influence of CCN (as for example aged AD) on cloud properties is unlikely, whereas clusters 1 and 2 represent conditions where CCN particles might have an effect on cloud properties.

4.3. Aerosol Indirect Effect

The droplet size distribution exerts two important indirect climate forcings (e.g., BAEDE 2007): (1) the effect that an increasing number of aerosol particles acting as CCN distributes the liquid water available in a cloud over a higher number of droplets that are smaller and increase cloud albedo, which in turn tends to lead to a climatic cooling; and (2) the cloud lifetime effect, which means that a shift towards smaller cloud droplets increases its lifetime due to decreased efficiency in producing rain from such clouds.

Clusters 1 and 2 were both subject to homogeneous mixing conditions where we could expect a dependency of droplet number concentration on the abundant aerosol concentration. As both clusters did not differ significantly in wind directions, we assume that there are no significant differences in abundant anthropogenic aerosols, which could be the reason for the different droplet sizes and number concentrations. There is additional evidence from the ATOFMS data that supports the link between periods, with AD transport and droplet number concentrations belonging to cluster 1 periods during which the dust counts exceed the counts of sea salt particles (Fig. 4a). Consequently, we conclude that long-range transported AD increased the amount of smaller droplets during our field campaign in a similar way as described by ROSENFELD et al. (2001) and KELLY et al. (2007). Most likely, soluble material partly condensed on the dust during the Atlantic passage, thereby increasing the ability of these dust particles to become CCN as expected under the aerosol indirect effect.

As with all statistical evidence, the question of causal relationship remains open and must be addressed in the future by performing specific, independent measurements that are able to clearly establish what the true role of AD really is. It would be essential to know whether these salts identified by ATOMFS form a coating on AD particles and generate processed aerosols that can act as CCN. This is important, because the general understanding is that dust particles normally act as ice nuclei and hence should not be very active in warm clouds such as those found at PE. Our measurements, including

the ATOMFS data, were unable to distinguish AD from other, possibly more local dust in the same air mass, and they cannot clarify the question whether sea-salt coexists with dust particles, or whether it coats them. Future studies should hence focus on this question, which must remain open in our study. Also, the role of interactions between dust particles and sea-spray salt needs to be investigated in more detail in the future.

5. Conclusions

Cloud properties are intimately linked to aerosol properties. Natural aerosols exist in the form of mineral dust particles from various sources: sea spray, volcanic ash, biological aggregates and many more. An important source of dust observed in Puerto Rico is of African origin, and particles are transported over long distances with the trade winds from Africa to the Caribbean. Hence, the episodic influx of such AD particles raises the question of whether these aerosols directly influence cloud properties, and also indirectly influence climate (via the aerosol indirect effect). If such a link is relevant for the Caribbean, one expects that an increase in CCN should lead to an increased number of cloud droplets, but of smaller drop size. We conclude that:

1. This is the first study that evaluated the relationship between long-range AD transport and cloud properties that are relevant for the cloud–albedo feedback in a tropical montane cloud forest, where vegetation response to changes in cloud properties are believed to be relevant.
2. We observed evidence for conditions with influence of AD on cloud properties in one out of three clusters; this was obtained by means of hierarchical cluster analysis of droplet size distributions measured at high time resolution.
3. Since this specific cluster represents conditions when AD was observed at the field site, we conclude that long-range transported AD can lead to more numerous cloud droplets in the TMCF at Pico del Este (Puerto Rico), which is similar to the anthropogenic aerosol indirect effect.

This holds under the assumption that cloud dynamics are slow, and hence clouds are homogeneously mixed. We argued that local air pollution sources are unlikely to have caused this statistical relationship during AD transport events, but recommend that future studies aim at obtaining independent measurements that are able to establish that this is not due to co-occurrence of AD and locally emitted aerosols, which are responsible for this finding.

References

ALLAN, J.D., BAUMGARDNER, D., RAGA, G.B., MAYOL-BRACERO, O.L., MORALES-GARCÍA, F., GARCIA-GARCIA, F., MONTERO-MARTINEZ, G., BORRMANN, S., SCHNEIDER, J., MERTES, S., WALTER, S., GYSEL, M., DUSEK, U., FRANK, G., KRÄMER, M. (2008) *Clouds and aerosols in Puerto Rico—A new evaluation*. Atmos. Chem. Phys. *8*, 1293–1309.

ANDREAE, M.O., ROSENFELD, D., ARTAXO, P., COSTA, A.A., FRANK, G.P., LONGO, K.M., SILVA-DIAS, M.A.F. (2004) *Smoking rain clouds over the Amazon*. Science *303*(5662), 1337–1342, doi:10.1126/science.1092779.

ANSMANN, A., MATTIS, I., MÜLLER, D., WANDINGER, U., RADLACH, M., ALTHAUSEN, D., DAMOAH, R. (2005), *Ice formation in Saharan dust over central Europe observed with temperature/humidity/aerosol Raman lidar*. J. Geophys. Res. *110*, D18S12, doi:10.1029/2004JD005000.

BAEDE, A. (2007) Glossary. In: SOLOMON, S., QIN, D., MANNING, M., MARQUIS, M., AVERYT, K., TIGNOR, M.M.B., MILLER JR., H.L., CHEN, Z. (eds) Climate Change 2007: The Physical Science Basis. Contribution of Working Group I to the Fourth Assessment Report of the Intergovernmental Panel on Climate Change, vol 463, Cambridge University Press, Cambridge, United

Kingdom and New York, NY, USA, Annex I, pp 941–954, doi:10.1038/463730a.

BAYNTON, H. (1969) *Ecology of an elfin forest in Puerto Rico 3. Hilltop and forest influences on microclimate of Pico del Este*. J. Arnold Arboretum *50*(1), 80–92.

BOUCHER, O., RANDALL, D., ARTAXO, P., BRETHERTON, C., FEINGOLD, G., FORSTER, P., KERMINEN, V.M., KONDO, Y., LIAO, H., LOHMANN, U., RASCH, P., SATHEESH, S.K., SHERWOOD, S., STEVENS, B., ZHANG, X.Y. (2013) Clouds and Aerosols, IPCC AR5, Chapter 7.

BRISTOW, C.S., HUDSON-EDWARDS, K.A., CHAPPELL, A. (2010), *Fertilizing the Amazon and equatorial Atlantic with West African dust*. Geophys. Res. Lett. *37*(14), L14,807, doi:10.1029/2010GL043486.

BROWN, S., LUGO, A., SILANDER, S., LIEGEL, L. (1983) Research History and Opportunities in the Luquillo Experimental Forest. Tech. rep., Gen. Tech. Rep. SO-44. U.S. Dept of Agriculture, Forest Service, Southern Forest Experiment Station., New Orleans, LA, USA.

BRUIJNZEEL, L.A., SCATENA, F.N., HAMILTON, L.S. (eds) (2010) Tropical Montane Cloud Forests: Science for Conservation and Management. Cambridge University Press, 740 pp.

BURKARD, R., EUGSTER, W., WRZESINSKY, T., KLEMM, O. (2002) *Vertical divergence of fogwater fluxes above a spruce forest*. Atmos. Res. *64*(1–4), 133–145, doi:10.1016/S0169-8095(02)00086-8.

CHOU, C., FORMENTI, P., MAILLE, M., AUSSET, P., HELAS, G., HARRISON, M., OSBORNE, S. (2008), *Size distribution, shape, and composition of mineral dust aerosols collected during the African Monsoon Multidisciplinary Analysis Special Observation Period 0: Dust and Biomass-Burning Experiment field campaign in Niger, January 2006*. J. Geophys. Res. *113*, D00C10, doi:10.1029/2008JD009897.

COLARCO, P.R., TOON, O., REID, J.S., LIVINGSTON, J.M., RUSSELL, P.B., REDEMANN, J., SCHMID, B., MARING, H., SAVOIE, D., WELTON, E., CAMPBELL, J., HOLBEN, B., LEVY, R. (2003), *Saharan dust transport to the Caribbean during PRIDE: 2. Transport, vertical profiles, and deposition in simulations of in situ and remote sensing observations*. J. Geophys. Res. *108*(D19), 8590, doi:10.1029/2002JD002659.

COZ, E., GÓMEZ-MORENO, F.J., CASUCCIO, G.S., ARTÍÑANO, B. (2010) *Variations on morphology and elemental composition of mineral dust particles from local, regional, and long-range transport meteorological scenarios*. J. Geophys. Res. *115*, D12,204, doi:10.1029/2009JD012796.

DEVENISH, B.J., BARTELLO, P., BRENGUIER, J.L., COLLINS, L.R., GRABOWSKI, W.W., IJZERMANS, R.H.A., MALINOWSKI, S.P., REEKS, M.W., VASSILICOS, J.C., WANG, L.P., WARHAFT, Z. (2012) *Droplet growth in warm turbulent clouds*. Quart. J. Roy. Meteor. Soc. *138*, 1401–1429, doi:10.1002/qj.1897.

EUGSTER, W., BURKARD, R., HOLWERDA, F., SCATENA, F., BRUIJNZEEL, L. (2006) *Characteristics of fog and fogwater fluxes in a Puerto Rican elfin cloud forest*. Agr. Forest. Meteorol. *139*(3–4), 288–306, doi:10.1016/j.agrformet.2006.07.008.

FIELD, P.R., MÖHLER, O., CONNOLLY, P., KRÄMER, M., COTTON, R., HEYMSFIELD, A.J., SAATHOFF, H., SCHNAITER, M. (2006) *Some ice nucleation characteristics of Asian and Saharan desert dust*. Atmos. Chem. Phys. *6*, 2991–3006, doi:10.5194/acp-6-2991-2006.

FORMENTI, P., RAJOT, J.L., DESBOEUFS, K., CAQUINEAU, S., CHEVAILLIER, S., NAVA, S., GAUDICHET, A., JOURNET, E., TRIQUET, S., ALFARO, S., CHIARI, M., HAYWOOD, J., COE, H., HIGHWOOD, E.

(2008), *Regional variability of the composition of mineral dust from western Africa: Results from the AMMA SOP0/DABEX and DODO field campaigns*. J. Geophys. Res. *113*, D00C13, doi:10.1029/2008JD009903.

GARCIA-MARTINO, A.R., WARNER, G.S., SCATENA, F.N., CIVCO, D.L. (1996) *Rainfall, runoff and elevation relationships in the Luquillo mountains of Puerto Rico*. Caribb. J. Sci. *32*(4), 413–423.

GARD, E., MAYER, J.E., MORRICAL, B.D., DIENES, T., FERGENSON, D.P., PRATHER, K.A. (1997) *Real-Time Analysis of Individual Atmospheric Aerosol Particles: Design and Performance of a Portable ATOFMS*. Anal. Chem. *69*(20), 4083–4091, doi:10.1021/ac970540n.

GIBSON, E.R., HUDSON, P.K., GRASSIAN, V.H. (2006), *Physicochemical properties of nitrate aerosols: implications for the atmosphere*. J. Phys. Chem. A *110*(42), 11,785–11,799, doi:10.1021/jp063821k.

GIODA, A., MAYOL-BRACERO, O.L., MORALES-GARCÍA, F., COLLETT, J., DECESARI, S., EMBLICO, L., FACCHINI, M.C., MORALES-DE JESÚS, R.J., MERTES, S., BORRMANN, S., WALTER, S., SCHNEIDER, J. (2008) *Chemical Composition of Cloud Water in the Puerto Rican Tropical Trade Wind Cumuli*. Water Air Soil Poll. *200*(1–4), 3–14, doi:10.1007/s11270-008-9888-4.

GIODA, A., MAYOL-BRACERO, O.L., SCATENA, F.N., WEATHERS, K.C., MATEUS, V.L., MCDOWELL, W.H. (2013) C*hemical constituents in clouds and rainwater in the puerto rican rainforest: Potential sources and seasonal drivers*. Atmos. Environ. *68*, 208–220.

GOUDIE, A., MIDDLETON, N. (2001) *Saharan dust storms: nature and consequences*. Earth-Sci. Rev. *56*(1–4), 179–204, doi:10.1016/S0012-8252(01)00067-8.

GULTEPE, I. (2008) Measurements of light rain, drizzle and heavy fog. In: Michaelides, S. (ed) Precipitation: Advances in measurement, estimation and prediction, Springer, pp 59–82.

GULTEPE, I., ISAAC, G.A. (1999) *Scale effects on averaging of cloud droplet and aerosol number concentrations: Observations and models*. Journal of Climate *12*, 1268–1279.

GUSTAFSSON, R.J., ORLOV, A., BADGER, C.L., GRIFFITHS, P.T., COX, R.A., LAMBERT, R.M. (2005) *A comprehensive evaluation of water uptake on atmospherically relevant mineral surfaces: DRIFT spectroscopy, thermogravimetric analysis and aerosol growth measurements*. Atmos. Chem. Phys. *5*, 3415–3421, doi:10.5194/acp-5-3415-2005.

GYAN, K., HENRY, W., LACAILLE, S., LALOO, A., LAMSEE-EBANKS, C., MCKAY, S., ANTOINE, R.M., MONTEIL, M.A. (2005) *African dust clouds are associated with increased paediatric asthma accident and emergency admissions on the Caribbean island of Trinidad*. Int. J. Biometeorol. *49*(6), 371–376, doi:10.1007/s00484-005-0257-3.

HARTMANN, D.L., TANK, A.M.K., RUSTICUCCI, M., ALEXANDER, L., BROENNIMANN, S., CHARABI, Y.A.R., DENTENER, F., DLUGOKENCKY, E., EASTERLING, D., KAPLAN, A., SODEN, B., THORNE, P., WILD, M., ZHAI, P. (2013) Observations: Atmosphere and Surface, IPCC AR5, Chapter 2.

HERICH, H., TRITSCHER, T., WIACEK, A., GYSEL, M., WEINGARTNER, E., LOHMANN, U., BALTENSPERGER, U., CZICZO, D.J. (2009) *Water uptake of clay and desert dust aerosol particles at sub- and supersaturated water vapor conditions*. Phys. Chem. Chem. Phys. *11*(36), 7759, doi:10.1039/b916865f.

HOLWERDA, F. (2005) Water and energy budgets of rain forests along an elevation gradient under maritime tropical conditions. Ph.D. thesis, Vrije Universiteit, Amsterdam, 167 pp.

HOLWERDA, F., BURKARD, R., EUGSTER, W., SCATENA, F.N., MEESTERS, A.G.C., BRUIJNZEEL, L.A. (2006) *Estimating fog deposition at a Puerto Rican elfin cloud forest site: comparison of the water budget and eddy covariance methods*. Hydrol. Process. *20*(13), 2669–2692, doi:10.1002/hyp.6065.

HUANG, J., ZHANG, C., PROSPERO, J.M. (2010) *African dust outbreaks: A satellite perspective of temporal and spatial variability over the tropical Atlantic Ocean*. J. Geophys. Res. *115*, D05202, doi:10.1029/2009JD012516.

KANDLER, K., SCHÜTZ, L., DEUTSCHER, C., EBERT, M., HOFMANN, H., JÄCKEL, S., JAENICKE, R., KNIPPERTZ, P., LIEKE, K., MASSLING, A., PETZOLD, A., SCHLADITZ, A., WEINZIERL, B., WIEDENSOHLER, A., ZORN, S., WEINBRUCH, S. (2009) *Size distribution, mass concentration, chemical and mineralogical composition and derived optical parameters of the boundary layer aerosol at Tinfou, Morocco, during SAMUM 2006*. Tellus B *61*(1), 32–50, doi:10.1111/j.1600-0889.2008.00385.x.

KANJI, Z.A., ABBATT, J.P.D. (2006) *Laboratory studies of ice formation via deposition mode nucleation onto mineral dust and n-hexane soot samples*. J. Geophys. Res. *111*, D16204, doi:10.1029/2005JD006766.

KAUFMAN, Y.J., TANRÉ, D., BOUCHER, O. (2002) *A satellite view of aerosols in the climate system*. Nature *419*, 215–223.

KELLY, J., CHUANG, C., WEXLER, A. (2007) I*nfluence of dust composition on cloud droplet formation*. Atmos. Environ. *41*(14), 2904–2916, doi:10.1016/j.atmosenv.2006.12.008.

LASKIN, A., IEDEMA, M.J., ICHKOVICH, A., GRABER, E.R., TARANIUK, I., RUDICH, Y. (2005) *Direct observation of completely processed calcium carbonate dust particles*. Faraday Discuss. *130*, 453, doi:10.1039/b417366j.

LEGENDRE, P., LEGENDRE, L. (1998) Numerical Ecology, 2nd edn. No. 20 in Developments in Environmental Modeling, Elsevier, Amsterdam, 853 pp.

LEVIN, Z., GANOR, E., GLADSTEIN, V. (1996) *The effects of desert particles coated with sulfate on rain formation in the eastern Mediterranean*. J. Appl. Meteor. *35*(9), 1511–1523, doi:10.1175/1520-0450(1996).

LEVIN, Z., TELLER, A., GANOR, E., YIN, Y. (2005) *On the interactions of mineral dust, sea-salt particles, and clouds: A measurement and modeling study from the Mediterranean Israeli Dust Experiment campaign*. J. Geophys. Res. *110*, D20202, doi:10.1029/2005JD005810.

LI, W.J., SHAO, L.Y. (2009) *Observation of nitrate coatings on atmospheric mineral dust particles*. Atmos. Chem. Phys. *9*(6), 1863–1871, doi:10.5194/acp-9-1863-2009.

LI, X., MARING, H., SAVOIE, D., VOSS, K., PROSPERO, J.M. (1996) *Dominance of mineral dust in aerosol light-scattering in the North Atlantic trade winds*. Nature *380*, 416–419.

LÜÖND, F., STETZER, O., WELTI, A., LOHMANN, U. (2010) *Experimental study on the ice nucleation ability of size-selected kaolinite particles in the immersion mode*. J. Geophys. Res. *115*, D14,201, doi:10.1029/2009JD012959.

MARING, H., SAVOIE, D., IZAGUIRRE, M., CUSTALS, L., REID, J.S. (2003) *Vertical distributions of dust and sea-salt aerosols over Puerto Rico during PRIDE measured from a light aircraft*. J. Geophys. Res. *108*(D19), 8587, doi:10.1029/2002JD002544.

MATSUKI, A., SCHWARZENBOECK, A., VENZAC, H., LAJ, P., CRUMEYROLLE, S., GOMES, L. (2010) *Cloud processing of mineral dust: direct comparison of cloud residual and clear sky particles during AMMA aircraft campaign in summer 2006.*

Atmos. Chem. Phys. *10*(3), 1057–1069, doi:10.5194/acp-10-1057-2010.

MUHS, D., BUSH, C., STEWART, K., ROWLAND, T., CRITTENDEN, R. (1990) *Geochemical evidence of Saharan dust parent material for soils developed on Quaternary limestones of Caribbean and western Atlantic islands*. Quaternary Res. *33*(2), 157–177, doi:10.1016/0033-5894(90)90016-E.

NOVAKOV, T., RIVERA-CARPIO, C., PENNER, J., ROGERS, C. (1994) *The effect of anthropogenic sulfate aerosols on marine cloud droplet concentrations*. Tellus B *46*(2), 132–141.

PROSPERO, J.M., LAMB, P.J. (2003) *African droughts and dust transport to the Caribbean: climate change implications*. Science *302*(5647), 1024–1027, doi:10.1126/science.1089915.

PROSPERO, J.M., MAYOL-BRACERO, O.L. (2013) *Understanding the transport and impact of african dust on the caribbean basin*. Bull. Amer. Meteorol. Soc. *94*, 1329–1337, doi:10.1175/BAMS-D-12-00142.1.

PROSPERO, J.M., NEES, R.T. (1986) *Impact of the North Afrcian drought and El Nino on mineral dust in the Barbados trade winds*. Nature *320*, 735–738.

PROSPERO, J.M., LANDING, W.M., SCHULZ, M. (2010) *African dust deposition to Florida: Temporal and spatial variability and comparisons to models*. J. Geophys. Res. *115*, D13304, doi:10.1029/2009JD012773.

ROSENFELD, D., RUDICH, Y., LAHAV, R. (2001) *Desert dust suppressing precipitation: a possible desertification feedback loop*. Proc. Natl. Acad. Sci. USA. *98*(11), 5975–5980, doi:10.1073/pnas.101122798.

ROSENFELD, D., LOHMANN, U., RAGA, G.B., O'DOWD, C.D., KULMALA, M., FUZZI, S., REISSELL, A., ANDREAE, M.O. (2008) *Flood or drought: how do aerosols affect precipitation?* Science *321*(5894), 1309–1313, doi:10.1126/science.1160606.

SHI, Y., ZHANG, J., REID, J.S., HOLBEN, B., HYER, E.J., CURTIS, C. (2011) *An analysis of the collection 5 MODIS over-ocean aerosol optical depth product for its implication in aerosol assimilation*. Atmos. Chem. Phys. *11*(2), 557–565, doi:10.5194/acp-11-557-2011.

SHINN, E.A., SMITH, G.W., PROSPERO, J.M., BETZER, P., HAYES, M.L., GARRISON, V., BARBER, R.T. (2000) *African dust and the demise of Caribbean coral reefs*. Geophys. Res. Lett. *27*(19), 3029–3032, doi:10.1038/252093f0.

SPIEGEL, J.K., ZIEGER, P., BUKOWIECKI, N., HAMMER, E., WEINGARTNER, E., EUGSTER, W. (2012) *Evaluating the capabilities and uncertainties of droplet measurements for the fog droplet spectrometer (FM-100)*. Atmos. Meas. Tech. *5*, 2237–2260, doi:10.5194/amt-5-2237-2012.

SULLIVAN, R.C., MOORE, M.J.K., PETTERS, M.D., KREIDENWEIS, S.M., ROBERTS, G.C., PRATHER, K.A. (2009) *Effect of chemical mixing state on the hygroscopicity and cloud nucleation properties of calcium mineral dust particles*. Atmos. Chem. Phys. *9*, 3303–3316, doi:10.5194/acp-9-3303-2009.

TAKAHAMA, S., LIU, S., RUSSELL, L.M. (2010) *Coatings and clusters of carboxylic acids in carbon-containing atmospheric particles from spectromicroscopy and their implications for cloud-nucleating and optical properties*. J. Geophys. Res. *115*, D01202, doi:10.1029/2009JD012622.

TANNER, E., KAPOS, V., FRANCO, W. (1992) *Nitrogen and phosphorus fertilization effects on Venezuelan montane forest trunk growth and litterfall*. Ecology *73*(1), 78–86.

TWOMEY, S. (1977) *The influence of pollution on the shortwave albedo of clouds*. J. Atmos. Sci. *34*(7), 1149–1152.

WARNER, J. (1969) *The microstructure of cumulus cloud. Part I. General features of the droplet spectrum.* Journal of Atmospheric Sciences *26*, 1049–1059.

WILKS, D. (2006) Statistical Methods in Atmospheric Schiences, 2nd edn. Academic Press, San Diego.

ZHANG, J., REID, J.S. (2006), *MODIS aerosol product analysis for data assimilation: Assessment of over-ocean level 2 aerosol optical thickness retrievals.* J. Geophys. Res. *111*(D22), D22207, doi:10.1029/2005JD006898.